TÜBİTAK

Turkish Journal of Agriculture and Forestry

http://journals.tubitak.gov.tr/agriculture/

Research Article

Turk J Agric For
(2022) 46: 762-780
© TÜBİTAK
doi:10.55730/1300-011X.3040

4E analysis of an underfloor heating system integrated to the geothermal heat pump for greenhouse heating

Fatih ÜNAL[1], **Ahmet Erhan AKAN**[2], **Bünyamin DEMİR**[3,*], **Kaan YAMAN**[4]

[1]Department of Mechanical Engineering, Faculty of Engineering, Mersin University, Mersin, Turkey
[2]Machinery and Metal Technology, Çorlu Vocational School, Namık Kemal University, Çorlu, Tekirdağ, Turkey
[3]Department of Mechanical Engineering, Faculty of Engineering, Mersin University, Mersin, Turkey
[4]Department of Mechanical Engineering, Faculty of Engineering, Mersin University, Mersin, Turkey

Received: 22.02.2022 • **Accepted/Published Online:** 21.05.2022 • **Final Version:** 03.10.2022

Abstract: In this study, 4E (energy, exergy, exergoeconomic, and exergoenvironmental) analysis of an underfloor heating system integrated with the geothermal heat pump of a greenhouse with a usage area of 90 m^2 has been made. When the results of the 4E analysis applied to the system and its elements were examined, the energy efficiency of the heating system in the winter months has been determined to be 77.85% and the exergy efficiency 30.61%. According to the results of exergoeconomic analysis, the levelized energy cost of the system has been determined as 0.894 $/h, the unit exergy cost as 0.826 $/h, and the exergoeconomic factor value as 51.12%. According to the results of the exergoenvironmental analysis, the part-based environmental impact of the system was 0.0910 mPts/s, the environmental impact value due to exergy was 0.1823 mPts/s, and the exergoenvironmental factor value was 37.77%. In addition, the equivalent CO_2 emission value that will occur if the heating requirement of the greenhouse is met with a natural gas boiler instead of a geothermal heat pump was investigated and a comparison was made between the two systems. Accordingly, it has been determined that the emission of 909.75 kg equivalent carbon dioxide to the environment will be prevented in the 4-month period, which is considered the heating season, by using the heat pump. As a result, the examined heating system has been evaluated as the effective system for heating the greenhouse, reducing energy consumption, and reducing emissions that cause environmental pollution.

Key words: Greenhouse, energy analysis, exergy analysis, exergoeconomic analysis, exergoenvironmental analysis, equivalent CO_2 emission

1. Introduction

Nowadays, with the rapid decrease of fossil fuel resources, energy price increases associated with this decrease, and increasing greenhouse effect of CO_2 emissions, the interest for the use of clean and renewable energy sources has been growing (Hepbasli and Utlu, 2004). Scientists' search for new energy production technologies with high efficiency and low emission that will solve the increasing energy demand and related environmental problems continue rapidly (Shirazi et al., 2012). Especially in recent years, one of the most important trends driving agriculture to make farming more efficient and sustainable is the exploitation of different technologies (Ünal et al., 2021; Dobrota et al., 2021). From these perspectives, it is thought that heat pump technologies will play an important role in the heating sector and therefore in the future of the agricultural energy system. In addition, the promotion of thermodynamically high-efficiency heat pump units will significantly reduce greenhouse gas emissions related to the heating sector. Reducing greenhouse gas emissions can be achieved by applying advanced exergy-based tools (Morosuk and Tsatsaronis, 2009; 2019; Tsatsaronis and Morosuk, 2016). Heat pumps are advantageous due to their high utilization efficiency compared to conventional heating and cooling systems and are used in many applications. There are two commonly used types of heat pumps. These are air source and ground source (geothermal) heat pumps (Dincer and Rosen, 2013). In addition, radiant systems have recently been used on walls, floors, or ceilings for both heating and cooling. Compared to conventional systems based on forced convection, which control the room air temperature by supplying hot or cold air to the space, radiant systems can achieve a more homogeneous temperature distribution and higher thermal comfort with less energy consumption. The systems used for this purpose provide the required thermal comfort conditions by using serpentine channels embedded in floors, walls, and ceilings through which hot and cold liquid passes. Since radiant systems require

* Correspondence: bd@mersin.edu.tr

very low energy use compared to conventional heating systems, they can potentially be combined with heat pump systems (Okamoto, 2010; Acikgoz et al., 2014; Myhren and Holmberg, 2008; Aldawi et al., 2013).

In recent years, a new strategy called exergy, exergoeconomic, and exergoenvironmental analysis has been developed (Tsatsaronis and Morosuk, 2008; 2009; Morosuk and Tsatsaronis, 2008). Accordingly, Mehrabadi and Boyaghchi (2019) conducted a comparative study for exergy, exergoeconomic, and exergoenvironmental analyses for a multibelt system in the northern regions of Iran. Mousavi and Mehrpooya (2020) evaluated a new gradual absorption-compression cooling system in terms of exergy, exergoeconomic, and exergoenvironmental aspects. Based on the results they obtained, they calculated the total exergy efficiency of the process as 69%. Montazerinejad et al. (2019) applied advanced exergy, exergoeconomic, and exergoenvironmental analyses to better understand the performance of the new solar-based combined cooling, heating, and power system they proposed. Ghorbani et al. (2020) conducted exergy, exergoeconomic, and exergoenvironmental analyses to better understand the interaction between the components of an integrated internal reforming solid oxide fuel cell-gas turbine and organic Rankine cycle system and the overall system. As a result, they showed that the total energy and exergy efficiencies for the optimal system were 49.42% and 46.83%, respectively. In addition, heat pump systems, exergy, realistic improvement potentials, and exergoeconomic have been analyzed from different points of view. Ozgener and Hepbasli (2005) examined the performance of the solar energy-assisted ground source heat pump system used for heating a greenhouse by exergy analysis in their study. Jia et al. (2017) modeled the heat transfer in the underfloor heating system for the greenhouse and stated that the underground root temperature plays a role in the efficient growth of plants. Lohani and Schmidt (2010) compared the energy and exergy efficiency of the conventional system with the GSHP and ASHP systems. Hepbasli (2011) compared three different heating models used in the heating of greenhouses by using the exergy model. Esen et al. (2007) examined the energy and exergy efficiency of a ground source heat pump system using a horizontal ground source heat exchanger. They stated the exergy efficiency value of the system as 67.7%. Unal and Temir (2014) and Unal et al. (2018) conducted an economic analysis of energy, exergy, and exergoeconomic for the heating and cooling season of a vertical type ground source heat pump system in Mardin Province of Turkey. Akbulut et al. (2016) carried out an exergoeconomic and exergoenvironmental analysis of vertical type ground source heat pump system integrated with wall heating system in the experimental area of Yıldız Technical University. Erbay and Hepbasli (2017) applied exergy and exergoeconomic analysis to a drying system operating with a ground source heat pump (GSHP). Harjunowibowo et al. (2021) used GSHP for greenhouse heating and cooling in their study. In addition, although there are many comprehensive studies and critical reviews on radiant heating and cooling systems (Stetiu, 1999; Imanari et al., 1999; Vangtook and Chirarattananon, 2010; Rhee and Kim, 2015; Zhao et al., 2016; Hu et al., 2012; Karmann et al., 2017; Zhang et al. 2020) in the literature, there are limited studies on integrated systems.

In this study, different from the studies in the literature, the actual data of a geothermal heat pump with a horizontal type heat exchanger and an integrated underfloor heating system during a 4-month heating period were taken. Using the data obtained from the experimental study, 4E (energy, exergy, exergoeconomic, and exergoenvironmental) analysis of the system and system elements defined for the heating process was performed, and the distribution of the losses in the system on the system elements was investigated separately. Using the data obtained, the CO_2 equivalent emission value that will occur if the greenhouse is heated by a natural gas system and the CO_2 equivalent emission that will be released to the environment by the heat pump system were compared. The results obtained were examined as a whole and while the efficiency, economic, and environmental evaluation of the system was made, the system elements were also compared with each other.

2. Materials and methods

The underfloor heating system integrated into the geothermal heat pump installed in a greenhouse located in İstanbul Province Silivri District was examined. Energy, exergy, exergoeconomic, and exergoenvironmental analyses were applied to the system by using the data of the experimental studies conducted during the winter season. The space used for the experiment is a greenhouse with a 90 m^2 usage area. The general scheme of the system used in the heating process is shown in Figure 1. In the system given in Figure 1, the heat ($\dot{Q}_G$), taken from the ground with a horizontal type underground heat exchanger (UHE) is transferred to the evaporator of the heat pump. Evaporator (EVA) draws heat ($\dot{Q}_L$) and turns this heat transfer fluid into gas. The temperature and pressure of the gaseous heat transfer fluid are increased by compression in the compressor (COMP) and the fluid is transported to the condenser (CON) of the heat pump. Here, the heat ($\dot{Q}_H$) arising during condensation is transferred to the accumulation tank (AT). Then the refrigerant passes through the throttling valve (TV) and the cycle continues. The heat ($\dot{Q}_{AT}$) transferred to the underfloor heating circuit through the accumulation tank is transmitted to the space through the underfloor heating panels (FHP) ($\dot{Q}_{FHP}$).

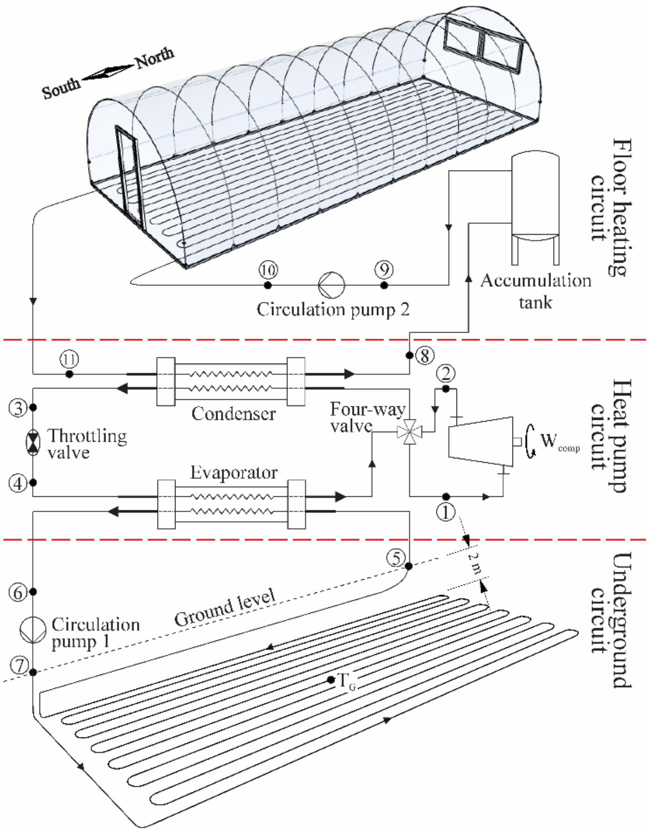

Figure 1. Floor plan of the greenhouse.

A geothermal heat pump system integrated into the underfloor heating system was used to meet the heating requirement of the determined test site. The system consists of three circuits: underground circuit (UHC), heat pump circuit (HPC), and underfloor heating circuit (FHC). The excavation was carried out in an area of 2 m deep, approximately 20 m long, and 5 m wide for the underground circuit (UHC). The underground heat exchanger (UHE), made of polyethylene pipes resistant to high operating pressure, was supplied in 100 m long coils. While the 350 m long heat exchanger was created using 4 coil pipes, the pipes were placed horizontally at a depth of 2 m and 40 cm gaps were left between the pipes. Radiant panels providing underfloor heating-cooling were used in the underfloor heating circuit. The catalog data of the geothermal heat pump is given in Table 1.

Measured variable parameters of the system are temperature, pressure, and flow values. Critical points are determined in the system flow chart (Figure 1) and the values for these points are recorded instantly with the datalogger device. Measuring instruments used in the experiments and their sensitivities are given in Table 2.

The theoretical and experimental acceptances for this study are listed below.

- The systems examined are real systems and conform to the steady-flow open system model. The materials are homogeneous and their standard properties were taken from the literature, and the nonmeasured properties of the devices were taken from the catalogue values. Analyses for the heating season were made based on the data recorded between 01.11.2020 and 28.02.2021.

- Heat loss was neglected since the underground heat exchanger was surrounded by the earth. ($\dot{Q}_{L,UHE} = 0$). There was no enthalpy loss in the throttle valve ($h_3 = h_4$).

- The heat pump system was purchased as a whole. Therefore, the costs of the analyzed parts of this system (compressor, condenser, throttling valve, and evaporator) were found by redistributing the total cost to the heat pump components in proportion to the actual costs. System life was taken as 20 years, repayment rate as 6%, interest rate as 3%, and escalation rate as 4%. The annual maintenance fee was set at \$ 150. During the analysis, the maintenance cost was added to the compressor from the system elements.

- A waste scenario and calculation were not created, assuming that the necessary improvements and part changes would be made and reused at the end of its life cycle.

- The cost of polyethene pipes was 3 \$/m.

Table 1. Catalogue data of the geothermal heat pump.

Model		Geothermal heat pump
10° / 35°	Heating capacity	12.10 kW
	Electricity consumption	2.69 kW
	Ampere	5.40 A
Maximum output temperature		60 °C
Water flow		2.17 m^3/h
Water connection		1 1/4"
Cooler liquid		R410A
Electric power		380/3/50 V/P/Hz
Compressor type		Scroll type

Table 2. Measuring instruments used in experiments and their sensitivities.

Measurement tool	Measuring place	Sensitivity
Tempsens / T-type thermocouple	In points 1 to 11, T_{in}, T_{out}, T_{at}, T_g, and T_{fh}	±0.25–0.5 °C
Testo 810 / Digital thermometer (infrared)	Surface temperature of the floor	±2.0 °C
Testo 511 / Absolute pressure meter	Air pressure	±0.003 bar
Delta OHM HD 2301 / Thermo-hygrometer	Air temperature	±0.5 °C
HP475ACIR / K-type probe	Air temperature and humidity	±0.3 °C, ±3%
Vf-Ect / Pressure transmitter / (0-40bar)	2, 3, 7, and 10	±0.5% mbar
Vf-Qtld / Turbine type flowmeter	7, 10	±0.5% m^3/h
Testo 770-3 / Current meter	Electricity grid	±1.0%, ± 1.5A
Expert Logger 200 / Data logger	Temperature, pressure, and flow	0.02%

- Each of the circulation pumps (P) used in the accumulation tank (AT), underground circuit (UHC), and underfloor heating circuit (FHC) cost $ 250.

- The storage tank had a capacity of 100 L and was made of stainless steel. The total cost of the storage tank was $ 1000, including connection pipes, insulation, and equipment.

- Radiant panels providing underfloor heating and cooling have been used in the underfloor heating circuit. In the panels, 700 m of 16 mm diameter and 25 m of 20 mm diameter polyethene pipe were used. Piping material, collectors and other connection equipment, labor, and plaster cost a total of $ 1000.

- Water was used as the heat carrier fluid in the underground and floor cooling system, and R410A was used as the refrigerant in the heat pump circuit. Thermophysical properties of water were taken from the EES program, and properties of R410A were taken from Solkane 8.0 and RefProp Version 10 package programs. The specific heat of water was 4.186 kJ/kg, environmental reference values were taken as T_0 = 0.01 °C and P_0 = 1 bar.

2.1. Energy and exergy analysis

The energy balance for the first law of thermodynamics is expressed by equation (1) (Dincer and Rosen, 2013).

$$\dot{E}_i - \dot{E}_e = \Delta\dot{E}_{sys} \tag{1}$$

In equation (1), $\dot{E}_i$ indicates the amount of energy entering the system per unit time, $\dot{E}_e$ the amount of energy leaving the system per unit time, and $\Delta\dot{E}_{sys}$ indicates the amount of energy change per unit time in the system. The energy balance of smooth flow balanced open systems is shown by equation (2).

$$\dot{E}_i = \dot{E}_e \tag{2}$$

Thus, the energy balance for the whole system can be calculated with the help of equation (2).

$$\dot{E}_i = \dot{Q}_G + \dot{W}_{p1} + \dot{W}_{comp} + \dot{W}_{p2} \tag{3}$$

$$\dot{E}_e = \dot{Q}_{FH} + \dot{Q}_L \tag{4}$$

$$\dot{Q}_G + \dot{W}_{p1} + \dot{W}_{comp} + \dot{W}_{p2} = \dot{Q}_{FH} + \dot{Q}_L \tag{5}$$

Generally, efficiency is obtained by dividing the desired value by the value that needs to be spent.

$$\eta = \frac{\text{fuel}}{\text{product}} \tag{6}$$

For the system, the first law of efficiency, i.e. the efficiency coefficient of the system in the heating process is calculated as follows:

$$COP_{H,sys} = \frac{\dot{Q}_{FH}}{\dot{W}_{p1} + \dot{W}_{comp} + \dot{W}_{p2}} \tag{7}$$

Exergy, on the other hand, is the part of the energy that does the work that is the usable energy. The specific flow exergy of the refrigerant or water is evaluated as (Dincer and Rosen, 2013);

$$ex_{r,w} = (h - h_0) - T_0(s - s_0) \tag{8}$$

where *h* is enthalpy, *s* is entropy, and the subscript zero indicates properties at the reference (dead) state (i.e. at P_o and T_o). If the total exergy flux is;

$$\dot{E}x = \dot{m}ex \tag{9}$$

Exergy amount lost per unit time for any element of the system Ex_L;

$$\dot{E}x_L = \dot{E}x_Q - \dot{E}x_{W,E} + \sum \dot{E}x_{mass,i} - \sum \dot{E}x_{mass,e} \tag{10}$$

or

$$\dot{E}x_L = \sum \left(1 - \frac{T_0}{T}\right)\dot{Q} - \dot{W} + \sum \dot{m}_i ex_i - \sum \dot{m}_e ex_e \tag{11}$$

It refers to the sum of the exergy flux transferred to the system and the exergy flux consumed due to irreversibility and cannot be used elsewhere. Exergy loss for the analyzed heating system can be written using equation (12).

$$\dot{E}x_{L,sys} = \dot{Q}_G\left(1 - \frac{T_0}{T_G}\right) + \dot{W}_{p1} + \dot{W}_{comp} + \dot{W}_{p2} - \dot{Q}_{FH} \times \left(1 - \frac{T_0}{T_{FH}}\right) \tag{12}$$

Exergy efficiency;

$$\eta_{II} = 1 - \frac{\dot{E}x_L}{\dot{E}x_{in}} = \frac{\dot{E}x_{product}}{\dot{E}x_{fuel}} \tag{13}$$

is expressed by the formula (13). Exergy efficiency can be calculated with equation (14), taking into account the efficiency of compressors and pumps.

$$\eta_{II,sistem} = \frac{\dot{Q}_G\left(1 - \frac{T_0}{T_G}\right)}{\dot{Q}_{FH}\left(1 - \frac{T_0}{T_{FH}}\right) + \dot{W}_{p1} + \dot{W}_{komp} + \dot{W}_{p2}} \tag{14}$$

Energy and exergy balances of all systems and components are given in Table 3.

2.2. Exergoeconomic and exergoenvironmental analysis

For exergoeconomic analysis, if the price of unit exergy is shown as "c", the total exergy price can be expressed by the following equation (Mehrabadi and Boyaghchi, 2019):

$$\dot{C} = c\dot{E}x = c(\dot{m}ex) \tag{15}$$

where $\dot{E}x$ is the exergy flux and $\dot{C}$ is the price of exergy flux. The following expression can be written by the above equation:

$$\dot{C}_k = c_k\dot{E}x_k = c_k(\dot{m}_k ex_k) \tag{16}$$

$$\dot{C}_w = c_w\dot{W} \tag{17}$$

$$\dot{C}_q = c_q\dot{E}x_q \tag{18}$$

While determining the exergy cost, the components in a system are handled separately. The cost balance equation for the k^{th} component of a system can be written as follows (Temir and Bilge, 2004).

$$\sum C_{e,k} + C_{w,k} = C_{q,k} + \sum C_{i,k} + Z_k \tag{19}$$

where Z_k is the monetary value brought to a value (levelized) that includes the investment, operation, and maintenance costs of the kth component of the system. This value (Z); annual working time is a function of parameters such as system life, interest, escalation (Temir and Bilge, 2004).

$$Z = A\left[\frac{\text{Initial investment cost}}{\text{System Life x Annual Working Hours}} + \frac{\text{Electricity + Maintenance Expensei}}{\text{Annual Working Hours}}\right] \tag{20}$$

While calculating the Z value; the sum of initial investment and operating costs corresponding to unit time is multiplied by the "bringing to a value factor (A)" The factor of bringing into a value is expressed in the following equation:

$$A = \frac{CELF}{1 + r_i} \tag{21}$$

In this equation, the "CELF" value is the Fixed Escalation Correction Factor, and the "r_i" value is the interest rate. The constant escalation correction factor is expressed in the following equation:

$$CELF = \frac{k(1 - k^n)}{1 - k}CRF \tag{22}$$

In the given equation, the "CRF" value indicates the capital recovery factor, the "k" value indicates the adjusted price correction factor, and the "n" value indicates the expected life for the system or component. The capital recovery factor (CRF) is expressed by the following equation:

$$CRF = \frac{i_{eff}(1 + i_{eff})^n}{(1 + i_{eff})^n - 1} \tag{23}$$

In the given equation, the "i_{eff}" value indicates the repayment rate. The price correction factor is expressed by the following equation:

$$k = \frac{(1 + r_n)}{(1 + i_{eff})} \tag{24}$$

Evaluations of the performance of a component are provided by the exergoeconomic factor defined for each

Table 3. Energy, exergy, exergoeconomic, and exergoenvironmental equations of systems and units.

Unit	Energy balance	Exergy balance	Exergoeconomic and exergoenvironmental equations
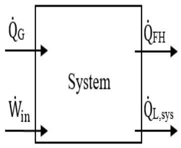	$\dot{Q}_G + \dot{W}_{p1} + \dot{W}_{comp} + \dot{W}_{p2} = \dot{Q}_{FH} + \dot{Q}_{L,sys}$ $COP_{H,sys} = \frac{\dot{Q}_{FH}}{\dot{W}_{p1} + \dot{W}_{comp} + \dot{W}_{p2}}$	$\dot{Ex}_G + \dot{W}_{p1} + \dot{W}_{comp} + \dot{W}_{p2} = \dot{Ex}_{FH} + \dot{Ex}_L$ $\eta_{II,H,sys} = \frac{\dot{Ex}_{FH}}{\dot{W}_{p1} + \dot{W}_{comp} + \dot{W}_{p2} + \dot{Ex}_G}$	$\dot{C}_{Q,G} + \dot{C}_{w,p1} + \dot{C}_{w,comp} + \dot{C}_{w,p2} + \dot{Z}_{sys} = \dot{C}_{Q,FH}$ $f_{C,H,system} = \frac{\dot{Z}_{sys}}{\dot{Z}_{sys} + (\dot{c}_{Q,FC} + \dot{c}_{w,in})\dot{Ex}_{L,sys}}$ $\dot{B}_{Q,G} + \dot{B}_{w,p1} + \dot{B}_{w,comp} + \dot{B}_{w,p2} + \dot{Y}_{sys} = \dot{B}_{Q,FH}$ $f_{B,H,system} = \frac{\dot{Y}_{sys}}{\dot{Y}_{sys} + (\dot{b}_{Q,FC} + \dot{b}_{w,in})\dot{Ex}_{L,sys}}$
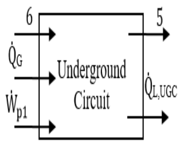	$\dot{E}_6 + \dot{Q}_G + \dot{W}_{p1} = \dot{E}_5 + \dot{Q}_{L,UGC}$ $\eta_{H,UGC} = \frac{\dot{E}_5 - \dot{E}_6}{\dot{W}_{p1} + \dot{Q}_G}$	$\dot{Ex}_6 + \dot{Ex}_G + \dot{W}_{p1} = \dot{Ex}_5 + \dot{Ex}_{L,UGC}$ $\eta_{II,H,UGC} = \frac{\dot{Ex}_5 - \dot{Ex}_6}{\dot{W}_{p1} + \dot{Ex}_G}$	$\dot{C}_6 + \dot{C}_{w,p1} + \dot{Z}_{UGC} = \dot{C}_{Q,G} + \dot{C}_5$ $f_{C,H,UGC} = \frac{\dot{Z}_{UGC}}{\dot{Z}_{UGC} + (\dot{c}_6 + \dot{c}_{w,p1})\dot{Ex}_{L,UGC}}$ $\dot{B}_6 + \dot{B}_{w,p1} + \dot{Y}_{UGC} = \dot{B}_{Q,G} + \dot{B}_5$ $f_{B,H,UGC} = \frac{\dot{Y}_{UGC}}{\dot{Y}_{UGC} + (\dot{b}_6 + \dot{b}_{w,p1})\dot{Ex}_{L,UGC}}$
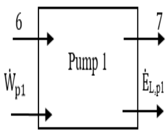	$\dot{E}_6 + \dot{W}_{p1} = \dot{E}_7 + \dot{E}_{L,p1}$ $\eta_{p1} = \frac{\dot{E}_7 - \dot{E}_6}{\dot{W}_{p1}}$	$\dot{Ex}_6 + \dot{W}_{p1} = \dot{Ex}_7 + \dot{Ex}_{L,p1}$ $\eta_{II,p1} = \frac{\dot{Ex}_7 - \dot{Ex}_6}{\dot{W}_{p1}}$	$\dot{C}_6 + \dot{C}_{w,p1} + \dot{Z}_{p1} = \dot{C}_7$ $f_{C,H,p1} = \frac{\dot{Z}_{p1}}{\dot{Z}_{p1} + \dot{c}_{w,p1}\dot{Ex}_{L,p1}}$ $\dot{B}_6 + \dot{B}_{w,p1} + \dot{Y}_{p1} = \dot{B}_7$ $f_{B,p1} = \frac{\dot{Y}_{p1}}{\dot{Y}_{p1} + \dot{b}_{w,p1}\dot{Ex}_{L,p1}}$

Table 3. (Continued).

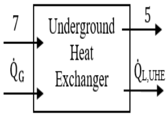	$\dot{E}_7 + \dot{Q}_G = +\dot{E}_5 + \dot{Q}_{L,UHE}$ $\eta_{H,UHE} = \frac{\dot{E}_5 - \dot{E}_7}{\dot{Q}_G}$	$\dot{E}x_7 + \dot{E}x_G = \dot{E}x_5 + \dot{E}x_{L,UHE}$ $\eta_{II,H,UHE} = \frac{\dot{E}x_5 - \dot{E}x_7}{\dot{E}x_T}$	$\dot{C}_7 + \dot{Z}_{UHE} = \dot{C}_5 + \dot{C}_{Q,G}$ $f_{C,H,UHE} = \frac{\dot{Z}_{UHE}}{\dot{Z}_{UHE} + \dot{c}_7\dot{E}x_{L,UHE}}$ $\dot{B}_7 + \dot{Z}_{UHE} = \dot{B}_5 + \dot{B}_{Q,G}$ $f_{B,H,UHE} = \frac{\dot{Y}_{UHE}}{\dot{Y}_{UHE} + \dot{b}_7\dot{E}x_{L,UHE}}$
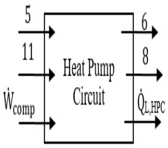	$\dot{E}_5 + \dot{W}_{comp} + \dot{E}_{11} =$ $\dot{E}_6 + \dot{E}_8 + \dot{Q}_{L,HPC}$ $\eta_{H,HPC} = \frac{\dot{E}_8 - \dot{E}_{11}}{\dot{W}_{comp} + \dot{E}_5 - \dot{E}_6}$	$\dot{E}x_5 + \dot{W}_{comp} + \dot{E}x_{11} = \dot{E}x_6 +$ $\dot{E}x_8 + \dot{E}x_{L,HPC}$ $\eta_{II,H,HPC} = \frac{\dot{E}x_8 - \dot{E}x_{11}}{\dot{W}_{comp} + \dot{E}x_5 - \dot{E}x_6}$	$\dot{C}_5 + \dot{C}_{w,comp} + \dot{C}_{w,p2} + \dot{C}_{11} + \dot{Z}_{HPC} = \dot{C}_6 +$ $\dot{C}_8$ $f_{C,H,HPC} = \frac{\dot{Z}_{HPC}}{\dot{Z}_{HPC} + (\dot{c}_5 + \dot{c}_{w,comp})\dot{E}x_{L,HPC}}$ $\dot{B}_5 + \dot{B}_{w,comp} + \dot{B}_{w,p2} + \dot{B}_{11} + \dot{Y}_{HPC} = \dot{B}_6 +$ $\dot{B}_8$ $f_{B,H,HPC} = \frac{\dot{Y}_{HPC}}{\dot{Y}_{HPC} + (\dot{b}_5 + \dot{b}_{w,comp})\dot{E}x_{L,HPC}}$
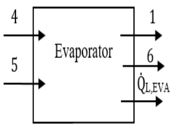	$\dot{E}_4 + \dot{E}_5$ $= \dot{E}_6 + \dot{E}_1 + \dot{Q}_{L,EVA}$ $\eta_{H,EVA} = \frac{\dot{E}_1 - \dot{E}_4}{\dot{E}_5 - \dot{E}_6}$	$\dot{E}x_4 + \dot{E}x_5 = \dot{E}x_6 + \dot{E}x_1 + \dot{E}x_{L,EVA}$ $\eta_{II,H,EVA} = \frac{\dot{E}x_1 - \dot{E}x_4}{\dot{E}x_5 - \dot{E}x_6}$	$\dot{C}_4 + \dot{C}_5 + \dot{Z}_{EVA} = \dot{C}_6 + \dot{C}_1$ $f_{C,H,EVA} = \frac{\dot{Z}_{EVA}}{\dot{Z}_{EVA} + \dot{c}_5\dot{E}x_{L,EVA}}$ $\dot{B}_4 + \dot{B}_5 + \dot{Y}_{EVA} = \dot{B}_6 + \dot{B}_1$ $f_{B,H,EVA} = \frac{\dot{Y}_{EVA}}{\dot{Y}_{EVA} + \dot{b}_5\dot{E}x_{L,EVA}}$
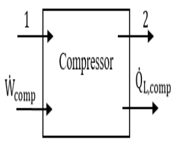	$\dot{E}_1 + \dot{W}_{comp}$ $= \dot{E}_2 + \dot{Q}_{L,comp}$ $\eta_{H,comp} = \frac{\dot{E}_2 - \dot{E}_1}{\dot{W}_{comp}}$	$\dot{E}x_1 + \dot{W}_{comp} = \dot{E}x_2 + \dot{E}x_{L,comp}$ $\eta_{II,H,comp} = \frac{\dot{E}x_2 - \dot{E}x_1}{\dot{W}_{comp}}$	$\dot{C}_1 + \dot{C}_{w,comp} + \dot{Z}_{comp} = \dot{C}_2$ $f_{C,H,comp} = \frac{\dot{Z}_{comp}}{\dot{Z}_{comp} + (\dot{c}_1 + \dot{c}_{w,komp})\dot{E}x_{L,comp}}$ $\dot{B}_1 + \dot{B}_{w,comp} + \dot{Y}_{comp} = \dot{B}_2$ $f_{B,H,comp} = \frac{\dot{Y}_{comp}}{\dot{Y}_{comp} + (\dot{b}_1 + \dot{b}_{w,komp})\dot{E}x_{L,comp}}$

Table 3. (Continued).

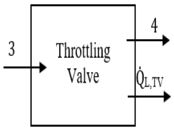	$\dot{E}_3 = \dot{E}_4 + \dot{Q}_{L,TV}$ $\eta_{H,TV} = \frac{\dot{E}_4}{\dot{E}_3}$	$\dot{E}x_3 = \dot{E}x_4 + \dot{E}x_{L,TV}$ $\eta_{II,H,TV} = \frac{\dot{E}x_4}{\dot{E}x_3}$	$\dot{B}_3 + \dot{Z}_{TV} = \dot{B}_4$ $f_{C,H,TV} = \frac{\dot{Z}_{TV}}{\dot{Z}_{TV} + \dot{c}_3\dot{E}x_{L,TV}}$ $\dot{B}_3 + \dot{Y}_{TV} = \dot{B}_4$ $f_{B,H,TV} = \frac{\dot{Y}_{TV}}{\dot{Y}_{TV} + \dot{b}_3\dot{E}x_{L,TV}}$
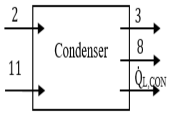	$\dot{E}_2 + \dot{E}_{11}$ $= \dot{E}_3 + \dot{E}_8 + \dot{Q}_{L,CON}$ $\eta_{H,CON} = \frac{\dot{E}_8 - \dot{E}_{11}}{\dot{E}_2 - \dot{E}_3}$	$\dot{E}x_2 + \dot{E}x_{11} = \dot{E}x_3 + \dot{E}x_8$ $+ \dot{E}x_{L,CON}$ $\eta_{II,H,CON} = \frac{\dot{E}x_8 - \dot{E}x_{11}}{\dot{E}x_2 - \dot{E}x_3}$	$\dot{C}_2 + \dot{C}_5 + \dot{Z}_{CON} = \dot{C}_3 + \dot{C}_6$ $f_{C,H,CON} = \frac{\dot{Z}_{CON}}{\dot{Z}_{CON} + \dot{c}_5\dot{E}x_{L,CON}}$ $\dot{B}_2 + \dot{B}_5 + \dot{Y}_{CON} = \dot{B}_3 + \dot{B}_6$ $f_{B,H,CON} = \frac{\dot{Y}_{CON}}{\dot{Y}_{CON} + \dot{b}_5\dot{E}x_{L,CON}}$
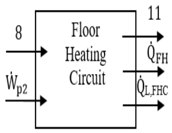	$\dot{E}_8 + \dot{W}_{p2}$ $= \dot{E}_{11} + \dot{Q}_{FH} + \dot{Q}_{L,FHC}$ $\eta_{H,FHC} = \frac{\dot{Q}_{FH}}{\dot{E}_8 - \dot{E}_{11} + \dot{W}_{p2}}$	$\dot{E}x_8 + \dot{W}_{p2} = \dot{E}x_{11} + \dot{E}x_{FH}$ $+ \dot{E}x_{L,FHC}$ $\eta_{II,H,FHC} = \frac{\dot{E}x_{FH}}{\dot{E}x_8 - \dot{E}x_{11} + \dot{W}_{p2}}$	$\dot{C}_8 + \dot{C}_{w,p2} + \dot{C}_{Q,FH} + \dot{Z}_{FHC} = \dot{C}_{11}$ $f_{C,H,FHC} = \frac{\dot{Z}_{FHC}}{\dot{Z}_{FHC} + (\dot{c}_{Q,FC} + \dot{c}_8)\dot{E}x_{L,FHC}}$ $\dot{B}_8 + \dot{B}_{w,p2} + \dot{B}_{Q,FH} + \dot{Y}_{FHC} = \dot{B}_{11}$ $f_{B,H,FHC} = \frac{\dot{Y}_{FHC}}{\dot{Y}_{FHC} + (\dot{b}_{Q,FH} + \dot{b}_8)\dot{E}x_{L,FHC}}$
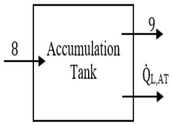	$\dot{E}_8 = \dot{E}_9 + \dot{Q}_{L,AT}$ $\eta_{H,AT} = \frac{\dot{E}_8}{\dot{E}_9}$	$\dot{E}x_8 = \dot{E}x_9 + \dot{E}x_{L,AT}$ $\eta_{II,H,AT} = \frac{\dot{E}x_8}{\dot{E}x_9}$	$\dot{C}_8 + \dot{Z}_{AT} = \dot{C}_9$ $f_{C,H,AT} = \frac{\dot{Z}_{AT}}{\dot{Z}_{AT} + \dot{c}_8\dot{E}x_{L,AT}}$ $\dot{B}_8 + \dot{Y}_{AT} = \dot{B}_9$ $f_{B,H,AT} = \frac{\dot{Y}_{AT}}{\dot{Y}_{AT} + \dot{b}_8\dot{E}x_{L,AT}}$

Table 3. (Continued).

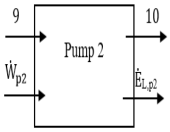	$\dot{E}_9 + \dot{W}_{p2} = \dot{E}_{10} + \dot{E}_{L,p2}$ $\eta_{p2} = \dfrac{\dot{E}_{10} - \dot{E}_9}{\dot{W}_{p2}}$	$\dot{E}x_9 + \dot{W}_{p2} = \dot{E}x_{10} + \dot{E}x_{L,p2}$ $\eta_{II,p2} = \dfrac{\dot{E}x_{10} - \dot{E}x_9}{\dot{W}_{p2}}$	$\dot{C}_9 + \dot{C}_{w,p2} + \dot{Z}_{p2} = \dot{C}_{10}$ $f_{C,H,p2} = \dfrac{\dot{Z}_{p2}}{\dot{Z}_{p2} + \dot{c}_{w,p2}\dot{E}x_{L,p2}}$ $\dot{B}_9 + \dot{B}_{w,p2} + \dot{Y}_{p2} = \dot{B}_{10}$ $f_{B,H,p2} = \dfrac{\dot{Y}_{p2}}{\dot{Y}_{p2} + \dot{b}_{w,p2}\dot{E}x_{L,p2}}$
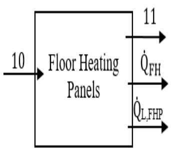	$\dot{E}_{10} = \dot{E}_{11} + \dot{Q}_{FH} + \dot{Q}_{L,FHP}$ $\eta_{H,FHP} = \dfrac{\dot{Q}_{FH}}{\dot{E}_{10} - \dot{E}_{11}}$	$\dot{E}x_{10} + \dot{E}x_{FH} = \dot{E}x_{11} + \dot{E}x_{L,FHP}$ $\eta_{II,H,FHP} = \dfrac{\dot{E}x_{FH}}{\dot{E}x_{10} - \dot{E}x_{11}}$	$\dot{C}_{10} + \dot{C}_{Q,FH} + \dot{Z}_{FHP} = \dot{C}_{11}$ $f_{C,H,FHP} = \dfrac{\dot{Z}_{FHP}}{\dot{Z}_{FHP} + \dot{c}_{Q,FH}\dot{E}x_{L,FH}}$ $\dot{B}_{10} + \dot{B}_{Q,FH} + \dot{Y}_{FHP} = \dot{B}_{11}$ $f_{B,H,FHP} = \dfrac{\dot{Y}_{FHP}}{\dot{Y}_{FCP} + \dot{b}_{Q,FH}\dot{E}x_{L,FH}}$

component. The exergoeconomic factor is expressed in the following equation for the kth component of the system (Bejan et al., 1996).

$$f_c = \frac{\dot{Z}}{\dot{Z} + c_p\dot{E}x_k} \tag{25}$$

The exergoeconomic balance of the whole system is shown with the help of equation (26) as follows:

$$\dot{C}_{Q,G} + \dot{C}_{W,comp} + \dot{C}_{W,p1} + \dot{C}_{W,p2} + \dot{Z}_{sys} = \dot{C}_{Q,FH} \tag{26}$$

The combination of an exergy analysis with a life cycle assessment (LCA) is a transformation of exergy economic analysis and is also referred to as external environment analysis (Buchgeister, 2010).

In this study, mass and energy balance for environmental analysis and life cycle assessment (LCA) for determining environmental effects based on this balance were used. The life cycle assessment (LCA) procedure based on Eco-indicator 99 to calculate environmental impacts is shown in Figure 2.

Life cycle analysis results defined by Eco-indicator 99 are matched with exergy currents. The environmental impact rate (b_j) per unit exergy for each flow (j) depends on the amount of environmental impact $\dot{B}_j$ and the amount of exergy ($\dot{E}x_j$) (Meyer et al., 2009).

$$b_j = \frac{\dot{B}_j}{\dot{E}x_j} \tag{27}$$

Environmental impacts associated with an inflow can be calculated directly. To calculate the input and output flow values, the functional relations between each system element (k) must be considered. Considering the environmental impact ($\dot{Y}_k$) based on element (k) as well as the environmental effect brought about by the exergy flow, the following correlations are obtained (Meyer et al., 2009):

$$\dot{Y}_k = \dot{Y}_k^{product} + \dot{Y}_k^{\text{operation}} + \dot{Y}_k^{\text{waste}} \tag{28}$$

$$\sum \dot{B}_{j,k,i} + \dot{Y}_k = \sum \dot{B}_{j,k,e} \tag{29}$$

Using the average unit environmental impact value of exergetic fuels for each part, the environmental impact value due to exergy loss is obtained as follows (Meyer et al., 2009):

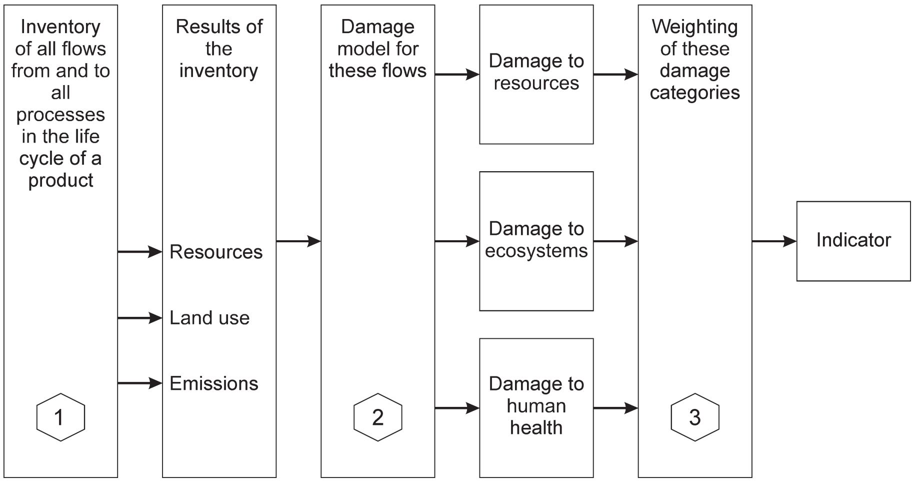

Figure 2. The general structure of LCA based on Eco-indicator 99 (Goedkoop and Spriensma, 2001).

$$\dot{B}_k = b_k \dot{Ex}_{L,k} \tag{30}$$

The ratio of part-based environmental impacts to total environmental impacts is comparable to exergoenvironmental factors (Meyer et al., 2009).

$$f_{B,k} = \frac{\dot{Y}_k}{\dot{Y}_k + \dot{B}_{yloss,k}} \tag{31}$$

The exergoenvironmental balance of the whole system is shown with the help of equation (32) as follows:

$$\dot{B}_{Q,G} + \dot{B}_{w,p1} + \dot{B}_{w,comp} + \dot{B}_{w,p2} + \dot{Y}_{sys} = \dot{B}_{Q,FH} \tag{32}$$

Exergoeconomic and exergoenvironmental equations belonging to all systems and components are given in Table 3.

2.3. Determining the heat demand rate of the greenhouse

To compare the CO_2 equivalent emission values of the heat pump system with the natural gas heating system, which is one of the traditional heating systems, the annual heating energy need of the examined greenhouse was calculated. In the greenhouse, the basis of all heat flow rates is heat losses by conduction and convection through the envelope, heat losses due to ventilation, and internal heat gain rates. Accordingly, the overall energy balance is as follows:

$$\dot{Q}_{net} = \sum \dot{Q}_{loss} - \sum \dot{Q}_{gain} \tag{33}$$

The rate of heat loss by conduction and convection through the envelope and heat losses due to ventilation of the greenhouse can be determined as follows (Hepbasli, 2013):

$$\dot{Q}_{net} = \sum_{i=1}^{n} \left(\frac{A_i}{R_i}\right) \Delta T f_w f_c f_s \tag{34}$$

where A and R respectively are the surface area and thermal resistance of the ith component. In this study, the glass-reinforced rigid polyester surface area is 307.02 m^2 and its thermal resistance is 0.1761 m^{2}K/W for the greenhouse. ΔT is the temperature difference between the inside and outdoor of the greenhouse. f_w, f_c, and f_s are the wind, the construction type, and the system factors, and they are equal to 1.13, 1.08, and 1.00, respectively.

Finally, the net specific heat rate is defined as:

$$\dot{q}_{net} = \frac{\dot{Q}_{net}}{A_{floor}} \tag{35}$$

where A_{floor} is the net floor area of the greenhouse.

2.4. Determination of the annual fuel consumption of the greenhouse and the equivalent CO_2 emission value

The annual heating energy need of the greenhouse is the energy requirement of the greenhouse that is assumed to be in continuous regime (22 °C indoor temperature) during the heating season (01.11.2020–28.02.2021). For this reason, it has been accepted that the system works continuously within the specified period. The fuel consumption (B_y) according to the annual heating energy need of the greenhouse has been calculated using equation (36):

$$B_y = \dot{Q}_{net}/(H_u \eta_k) \tag{36}$$

In equation (36), H_u refers to the lower heating value of the fuel (natural gas) used (H_u=34526.2 kJ/m^3), and η_k refers to the boiler efficiency (95%).

Eighty-five percent of the waste gases released as a result of burning fossil-based fuels used for heating purposes is CO_2. Therefore, CO_2 emission is taken into account in emission values. Depending on the net energy consumption of a greenhouse, the annual CO_2 emission amount according to the type of fuel used can be calculated with the help of equation (37) (Yazici, 2011).

$$SEGM_y = 0.278x10^{-3} B_y H_u FSEG \tag{37}$$

$SEGM_y$ in equation (37) is annual CO_2 emission (kg equivalent CO_2) and FSEG is the CO_2 emission conversion coefficient according to the fuel type. This value is 0.234 kg equivalent CO_2/kWh for natural gas and 1.009 kg equivalent CO_2/kWh for electricity.

2.5. Uncertainty analysis

The error analysis in this study was calculated using equation (38) developed by Kline and McClintock, based on the following assumptions, using the experimental devices placed at the locations shown in Figure 1 and the sensitivity values presented in Table 2.

$$W_R = \left[\left(\frac{\partial R}{\partial x_1} w_{x_1}\right)^2 + \left(\frac{\partial R}{\partial x_2} w_{x_2}\right)^2 + \cdots \left(\frac{\partial R}{\partial x_n} w_{x_n}\right)^2\right]^{\frac{1}{2}} \quad (38)$$

The following assumptions were taken into account in the experimental error analysis.

1- The experimental system is a system that is installed by the standards and operates under real operating conditions.

2- The calibration of the measuring devices used in the experiments is up-to-date and correct.

3- The measuring devices have no manufacturing defects.

4- The identified errors include constant and random errors.

In equation (38), R, x_1, x_2, …, x_n is a given function of the independent variables, w_1, w_2, …, w_n are the uncertainty of the independent variables.

The values obtained as a result of the calculations are presented in Table 4.

As can be seen from Table 4, it has been determined that the greatest error value that may occur during the experiments can occur during temperature measurements and these values are among the acceptable values. The measurements were evaluated with the uncertainty analysis (Acar and Arslan, 2017).

3. Results and discussions

The geothermal heat pump system integrated with the underfloor heating system consists of 3 circuits and 9 units. The flow rate, pressure, temperature, enthalpy, and entropy values of the determined nodal points of the geothermal heat pump system given in Figure 1 are given in Table 5. In addition, the energy and exergy values calculated by the equations given in Section 3 using these values are given in Table 6.

In this study, all analyses were made by applying the values given in Table 5 to the equations given in Table 3 for control volumes determined on the system depending on the acceptances.

3.1. Evaluation of energy and exergy analyses

To compensate for the heat loss in the test area during the examined process, depending on the measured outside air temperature, water at a temperature of 32.50–33.25 °C has been prepared in the accumulation tank. In this process, the electrical power consumed by the compressor and two circulation pumps was measured as 2.119 kW on average. The amount of energy that the system transfers to the test area has been relatively more affected by the change in outdoor temperature. It has been measured that this value varies between 9.31 and 9.47 kW. As a result of the energy analysis, it was seen that the operation of the system was affected by the outside temperature. Accordingly, the average COP value of the whole system was determined to be 4.09. Although the COP value of the heat pump device was found to be 4.88, when the system was examined as a whole, it was found that the COP value fell to 4.09. For the heating process, the results obtained from the energy and exergy analysis of the geothermal heat pump system integrated into the underfloor heating system and system elements are given in Table 6.

When Table 6 is examined, it can be seen that the amount of energy loss occurring in the heating system is 2.465 kW and the energy efficiency of the system is 77.85%. The amount of energy loss in the system units was determined as 0.721 kW in in-floor heating panels, 0.536 kW in the compressor, and 0.522 kW in the condenser, respectively. The element of the system with the lowest energy efficiency was determined as the compressor with 73.13%. Since the underground heat exchanger and throttle

Table 4. Total errors that may occur in experiments.

Error constituents parameters	Total error	Unit
Probable errors in temperature measurement	±1.03 to ±1.91	°C
Probable errors in pressure measurement	±0.51	mbar
Probable errors due to flow measurement	±0.87	m^3/h
Probable errors in electricity grid voltage measurement	±0.015	V
Probable errors in electricity grid current measurement	±0.03	A
Probable errors in the humidity measurement	±0.035 to ±0.042	%
Probable errors in the time measurement	±0.14	s
Other errors	±0.1 to ±0.2	%

Table 5. Determined values for nodal points in the heating process.

Node	Phase	m (kg/s)	P (bar)	T (°C)	h (kJ/kg)	s (kJ/kgK)	$\dot{E}$(kW)	$\dot{E}_x$ (kW)
1	Gas	0.048	10	9.45	429.37	1.8074	20.610	3.342
2	Liquid	0.048	18	58.34	459.85	1.8411	22.073	4.363
3	Wet vapor	0.048	18	25.63	245.62	1.1515	11.790	3.122
4	Gas	0.048	10	1.82	245.62	1.1557	11.790	3.067
5	Liquid	0.52	1.52	9.38	39.767	0.1421	20.679	0.516
6	Liquid	0.52	1.52	5.28	22.344	0.0816	11.619	0.049
7	Liquid	0.52	1.52	5.31	22.439	0.0816	11.668	0.099
8	Liquid	0.33	1.47	33.12	138.56	0.4792	45.725	2.543
9	Liquid	0.33	1.47	32.61	137.28	0.4753	45.302	2.472
10	Liquid	0.33	1.47	32.65	137.42	0.4753	45.349	2.518
11	Liquid	0.33	1.47	25.91	108.98	0.3826	35.963	1.489

Table 6. Average energy and exergy values of the system and its units.

Item	SYS	COMP	COND	EVA	TV	P1	UHE	P2	AT	FHP
$\dot{E}_i$ (kW)	11.130	22.609	58.036	32.469	11.790	11.679	20.679	45.362	45.725	45.349
$\dot{E}_e$ (kW)	8.664	22.073	57.515	32.229	11.790	11.668	20.679	45.349	45.302	44.628
$\dot{E}_L$ (kW)	2.465	0.536	0.522	0.240	0.000	0.011	0.000	0.014	0.422	0.721
$\dot{E}_f$ (kW)	11.130	1.999	10.283	9.060	11.790	0.060	9.011	0.060	45.725	9.385
$\dot{E}_p$ (kW)	8.664	1.463	9.761	8.820	11.790	0.049	9.011	0.046	45.302	8.664
η_I (%)	77.85	73.18	94.93	97.35	100.00	82.33	100.00	77.00	99.08	92.32
$\dot{E}x_i$ (kW)	2.699	5.342	5.853	3.583	3.122	0.109	0.678	2.532	2.543	2.518
$\dot{E}x_e$ (kW)	0.826	4.363	5.665	3.392	3.067	0.099	0.516	2.518	2.472	2.315
$\dot{E}x_L$ (kW)	1.873	0.978	0.188	0.191	0.055	0.011	0.162	0.014	0.071	0.203
$\dot{E}x_f$ (kW)	2.699	1.999	1.242	0.467	3.122	0.060	0.580	0.060	2.543	1.029
$\dot{E}x_p$ (kW)	0.826	1.021	1.054	0.275	3.067	0.049	0.417	0.046	2.472	0.826
η_{II} (%)	30.61	51.08	84.89	59.02	98.24	82.33	71.98	77.00	97.21	80.28

valve are considered without loss, there is no energy loss. The energy loss of the pumps in the system is very low. The exergy loss amount of the system was determined as 1.873 kW and the exergy efficiency as 30.61%. According to the results of the exergy analysis, it was determined that the unit with the lowest efficiency and the most exergy loss was the compressor. Accordingly, the working conditions, ambient conditions, and energy transfer evaluation of the heating system are given in Figure 3.

When Figure 3 is examined, the outdoor temperature and relative humidity were measured as an average of 5.92 °C and 89.46% in January, respectively. These values were measured as an average of 11.16 °C and 88.12% in November, respectively. The room temperature of the heated environment was adjusted to 22 °C set value throughout the entire heating period and it was tried to be kept at the same temperature continuously. The soil temperature at 2 m depth was measured as an average of 18.63 °C in January, an average of 18.83 °C in November and an average of 18.97 °C during the heating process. In this context, it has been observed that the amount of energy transferred from the soil to the system changes between 8.94 and 9.10 kW according to the outside temperature because of measurements and calculations.

In Figure 4, the distribution of monthly average energy and exergy loss amounts for the system and its units

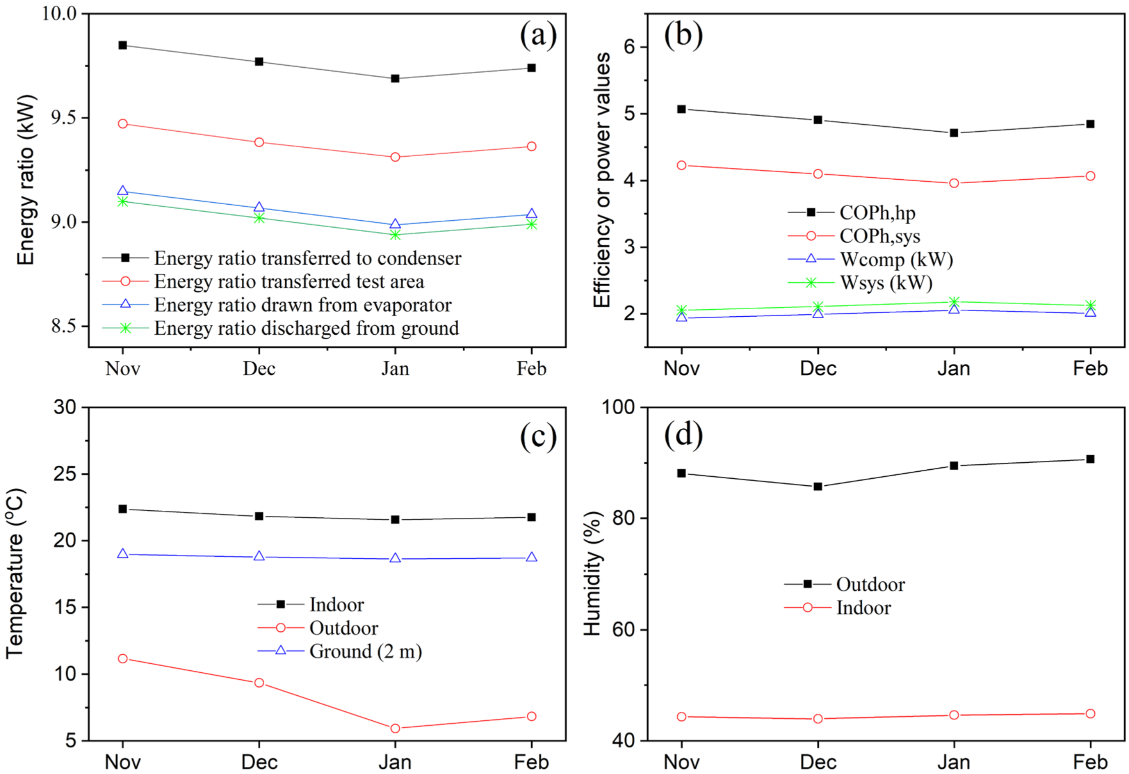

Figure 3. Energy analysis assessment of the system: (a) energy ratio obtained for the system, (b) efficiency and power consumption, (c) weather conditions, and (d) humidity conditions.

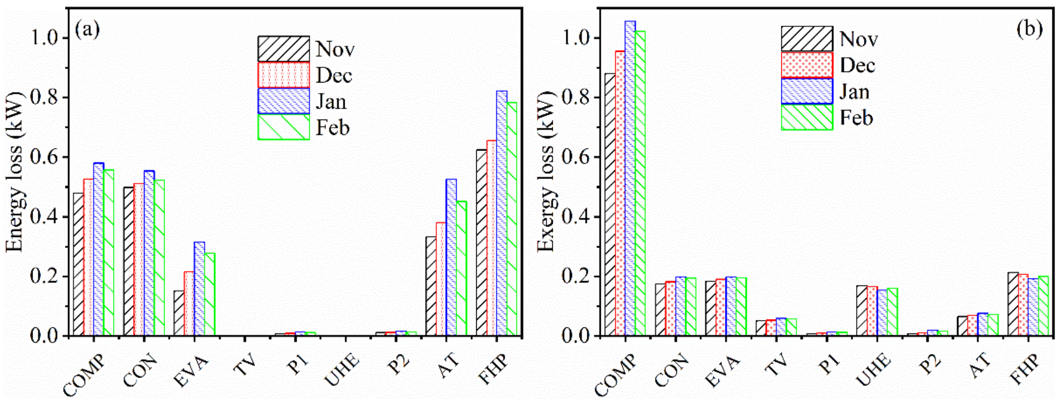

Figure 4. Monthly average (a) energy and (b) exergy loss distribution in the heating process.

is given. When Figure 4 is examined, according to the assumptions and calculations, energy and exergy losses are not dependent on the outside temperature for the throttle valve. For the other elements, it has been observed that, generally, the air temperature changes in the same direction, while the exergy loss in in-floor heating panels changes inversely with the outside air temperature. While the compressor is determined as the unit with the most serious exergy loss in the system, the underfloor heating panel, evaporator, condenser, and underground heat exchanger follow the compressor.

3.2. Evaluation of exergoeconomic and exergoenvironmental analyses

In the work done in this section, the exergoeconomic analysis includes the values of the levelized cost, the exergy cost, the exergoeconomic factor, and the exergy loss ratio, which is an important factor in the evaluation of the system. Exergoenvironmental analysis includes unit-based environmental impact, exergy-based environmental impact and exergy environmental factor values. With the help of the equations given in Table 3 prepared for the heating system and its elements, the results of exergoeconomic and exergoenvironmental analysis are given in Table 7.

When Table 7 is examined, the levelized cost value of the system used in the heating process was determined as 0.894 $/h and the environmental impact value on a unit basis was determined as 0.0910 mPts/s. In the process examined, the exergy economic factor value of the system was 51.12% and the exergy environmental factor value was 37.77%. According to the assumptions and calculations made for the heating system elements, the highest value of the total cost (levelized cost) was 0.171 $/h and the highest part-based environmental impact value was found in the compressor with 0.0351 mPts/s. The compressor has been determined as the heating system element with the lowest values of 30.19% and 24.99% exergoeconomic factor and exergoenvironmental factor, respectively. Figure 5 shows the monthly average exergy cost distribution of the system elements in the heating process. When Figure 5 is analyzed, the effects of climate change on exergy costs are also seen.

Figure 5 shows the monthly average exergy cost change in the system elements. This value changes depending on the change in outdoor temperature. According to the assumptions and calculations, this value was taken as "zero" for soil exergy. Examining the monthly average exergy cost distributions for the system elements, a change in the opposite direction with the outside air temperature for floor heating panels and throttle valve, while a change in the same direction with the air temperature was observed for other system elements. The element of the system with the highest exergy cost was determined as the element compressor with an average of 0.395 $/h. In Figure 6, the distribution of the monthly average exergoeconomic factor values of the system elements in the heating process is given.

In Figure 6, when the monthly exergy economic factor values of the system elements are examined, it is seen that this value changes depending on the outside temperature. For the throttle valve and floor heating panels, there was an exergoeconomic factor change in the opposite direction to the outdoor temperature, while the exergoeconomic factor value for other system elements has changed in the same direction with the outside air temperature. There is a direct relationship between the total cost brought to a value (levelized cost) and exergoeconomic factor values. In this context, the exergy economic factor value should be considered an important evaluation criterion in the improvements planned to be made on the system or system elements or in the design of new systems. System elements with low exergoeconomic factor value should be preferred primarily in improvements to be made to increase system efficiency. In the analysis, the element of the system with the lowest exergoeconomic factor was determined as the compressor for all months examined during the heating season. Figure 7 shows the monthly average exergy loss rate values of the system elements in the heating process.

When Figure 7 is examined, the element of the system with the highest rate of exergy loss in all months is the compressor. According to the results obtained during the heating process of the compressor, the exergy loss rate was determined to be 52.23% on average. As a result of the analysis, it has been seen that more than half of the exergy loss in the system occurred in the compressor. For all system elements, the exergy loss rate has changed in the same direction with the change in outdoor temperature.

When Figure 8 is examined, the element of the system with the highest exergy-based environmental impact value in all months is the compressor. The compressor is followed by condenser, evaporator, and underfloor heating panels, respectively. For all system elements, exergy-based environmental impact values change in the same direction with the change of outdoor air temperature, while this value has changed in the opposite direction with the outside air temperature in in-floor heating panels and throttle valves. In Figure 9, the change of average exergoenvironmental factor values of the system elements for the months examined during the heating process is given.

Table 7. Average exergoeconomic and exergoenvironmental analysis results.

Item	SYS	COMP	COND	EVA	TV	P1	UHE	P2	AT	FHP
$\dot{Z}$ ($/h)	0.894	0.171	0.138	0.138	0.039	0.025	0.145	0.025	0.082	0.131
$\dot{C}$ ($/h)	0.826	0.395	0.157	0.103	0.018	0.006	0.083	0.004	0.015	0.044
$f_{C,H}$ (%)	51.12	30.19	46.79	57.22	68.85	79.69	63.46	85.80	84.32	75.02
y_L (%)	100.00	52.23	10.02	10.21	2.94	0.57	8.67	0.74	3.78	10.84
$\dot{Y}$ (mPts/s)	0.0910	0.0351	0.0085	0.0085	0.0027	0.0022	0.0089	0.0022	0.0052	0.0178
$\dot{B}$ (mPts/s)	0.1823	0.1054	0.0164	0.0167	0.0048	0.0001	0.0053	0.0002	0.0068	0.0266
$f_{B,H}$ (%)	37.77	24.99	34.15	33.72	36.01	93.62	62.62	91.85	43.37	40.03

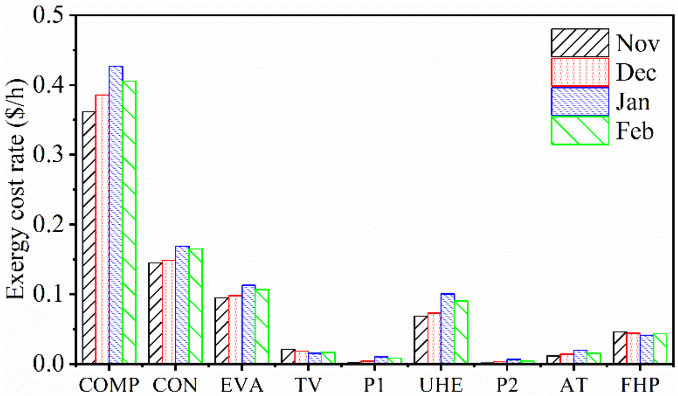

Figure 5. Monthly exergy cost distribution of system elements.

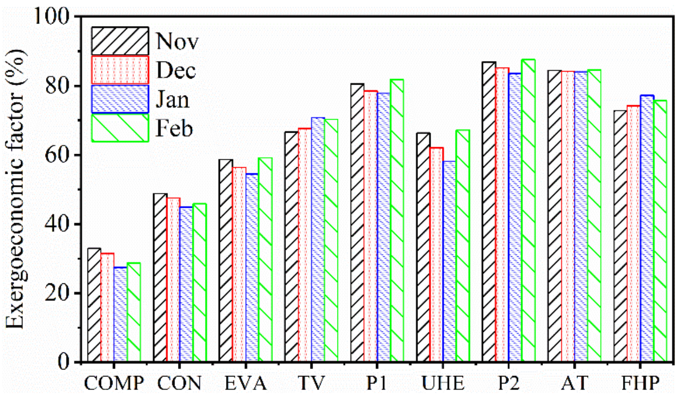

Figure 6. Monthly exergoeconomic factor distribution of system elements in the heating process.

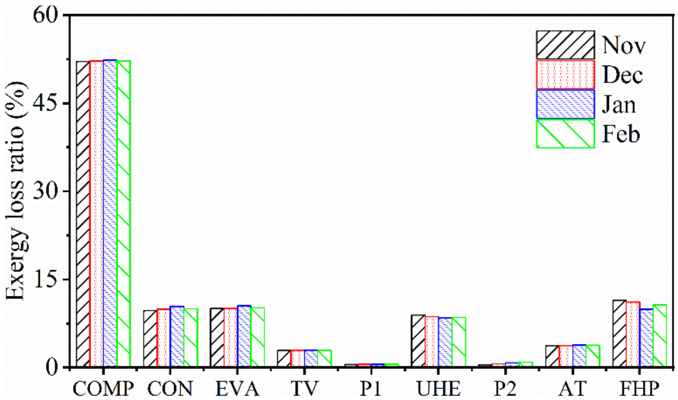

Figure 7. Distribution of monthly exergy loss rate of system elements.

Figure 9 shows the change of monthly exergoenvironmental factor values of the system elements. During the heating period, the element of the system with the lowest exergoenvironmental factor value in all months is the compressor. The compressor is followed by the evaporator, condenser, and underfloor heating panels. While the exergoenvironmental factor values for all system elements show a change in the same direction with the change of outdoor air temperature, this value has changed in the opposite direction with the outside air temperature in in-floor heating panels and throttle valve.

3.3. Evaluation of annual heating energy requirement analyses

By using the formulas presented in Section 2.3, specific heat loss values to be realized in the greenhouse were calculated. The heating energy requirement of the greenhouse

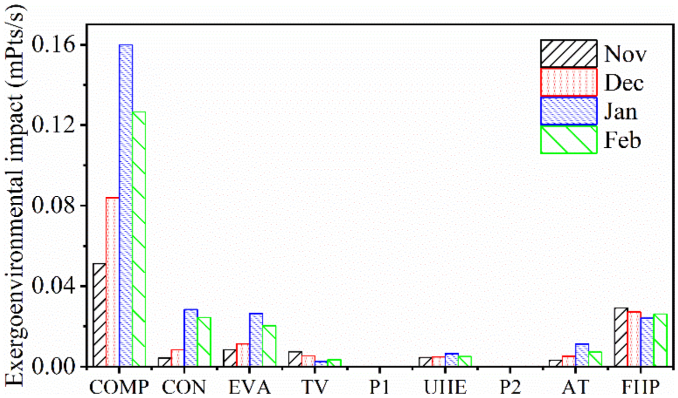

Figure 8. Monthly exergy-based environmental impact distribution of system elements.

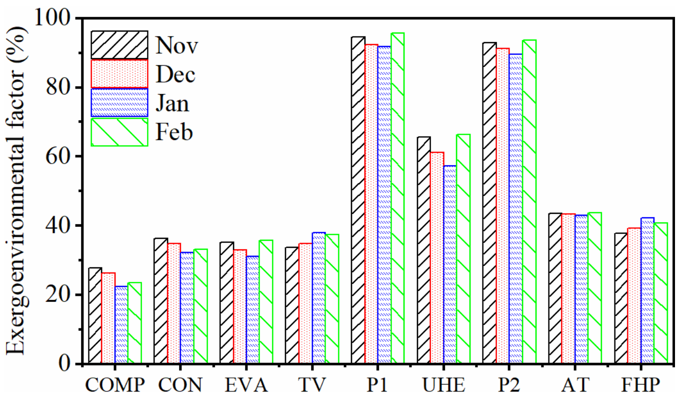

Figure 9. Monthly exergoenvironmental factor distribution of system elements.

Table 8. Heating energy needs monthly.

Months	Specific heat loss (W/K)	Temp. diff. (°C)	Heat loss (W)	Heat gain (W)	Heating energy requirement (kJ)
Nov	832.20	10.5	8738	3840.76	12,693,802
Dec		15.2	12649	4174.54	21,967,044
Jan		16.1	13398	4257.9	23,692,228
Feb		14.6	12150	4245.45	20,488,775

monthly during the heating season is presented in Table 8. As can be seen in Table 8, the total specific heat loss in the greenhouse was found to be 832.2 W/K. As a result of the calculations, the annual heating energy need of the greenhouse has been determined as 78,842 MJ.

3.4. Evaluation of equivalent carbon dioxide emission analyses

After the annual heating energy need of the greenhouse is calculated, it has been determined that if the greenhouse is heated by a natural gas boiler (η = 0.95) with the help of the equation (36), it will consume 2403.72 m^3 natural gas annually. After determining the amount of fuel required for the heating season, the equivalent amount of CO_2 amounts to be released to the environment by the heating systems compared with the help of equation (37) has been determined. Accordingly, it has been determined that the heat pump system will cause 4489 kg equivalent CO_2 emission during the heating season, while the natural gas heating system will cause 5398.75 kg equivalent CO_2 emission. As a result, the emission of 909.75 kg equivalent carbon dioxide to the environment will be prevented during the 4 months, which is regarded as the heating season, by using a heat pump.

4. Conclusions

In this study, 4E (energy, exergy, exergy-economic, and exogenous) analysis has been performed on the geothermal heat pump and system elements integrated into the underfloor heating system during the heating duration. The results obtained from the analyses are presented below.

1- As a result of the energy and exergy analyses, it was seen that the system operation was affected by the outside air temperature. Accordingly, the average COP value of the whole system was determined to be 4.09. The COP value found showed that the performance of the system gave close results to the studies examined in the literature, while it gave relatively better results than many systems. The reason for this has been determined as the radiant floor heating-cooling systems provide the desired thermal comfort at much lower temperatures when supported by the geothermal heat pump. The energy efficiency of the system was found to be 77.85% and the exergy efficiency was 30.61%. According to the results of the energy and exergy analysis, it was determined that the system is usable, but still, the system elements have improvement potential.

2- When the results of the analysis are examined, the cost value of the system in the heating process is 0.894 $/h, the environmental impact value on a piece basis is 0.0910 mPts/s, the exergoeconomic factor value is 51.12% and the exergoenvironmental factor value is 37.77%. According to the assumptions and calculations made for the heating system elements, the total levelized cost was 0.171 $/h and the highest part-based environmental impact value was seen in the compressor with 0.0351 mPts/s. The compressor was determined as the lowest heating system element with 30.19% and 24.99% exergoeconomic factor and exergoenvironmental factor values, respectively. In addition, the exergy loss rate of the compressor was found to be 52.23%. Therefore, the compressor should be considered first for the improvements to be considered. Thus, the efficiency of the system will be increased by reducing electricity consumption. To reduce electricity consumption, the operating range of the compressor can be narrowed or frequency-controlled compressors can be preferred. In addition, the improvements to be made in the insulation of the system elements and the space will enable the compressor to be less engaged, and the heat pump will be able to work longer in lower temperature regimes.

3- If the studied greenhouse is heated with a natural gas heating system, which is one of the traditional heating systems instead of the heat pump system, the equivalent CO_2 emission amount to be emitted to the environment was determined and compared with the heat pump system. Accordingly, it has been determined that the heat pump system will prevent 909.75 kg equivalent CO_2 emission in the heating season compared to the natural gas system.

As a result, our system is very effective in reducing energy consumption and greenhouse gas emissions. It is considered appropriate to use the system for İstanbul and provinces with similar climatic characteristics. However, it has been observed that using systems that provide high thermal comfort at low temperatures will be beneficial both economically and environmentally.

SYMBOLS

A	Area (m^2)
$\dot{C}$	Energy cost ($/h)
c	Unit exergy cost ($/kJ)
c_p	Specific heat (kJ/kg°C)
E	Energy (kJ)
$\dot{E}$	Energy flux (kW)
$\dot{E}x$	Exergy flux (kW)
$\dot{E}x_L$	Exergy loss (kW)
f	Exergoeconomic factor
h	Heat convection coefficient (W/m^2K), Enthalpy (kJ/kg)
i	Effective interest rate (%)
k	Levelized cost correction factor
$\dot{m}$	Mass flow rate (kg/s)
Q	Heat energy (kJ)
$\dot{Q}$	Heat flux (kW)
R	Thermal resistance (W/m^2K), Correction factor (-)
ri	Determined interest rate (%)
rn	Nominal escalation value (%)
S	Entropy (kJ/K)
s	Unit entropy (kJ/kgK)
T, t	Temperature (K), time (s)
U	Internal energy (kJ)
u	Unit internal energy (kJ/kg)
V	Volume (m^3)
v	Speed (m/s)
W	Work (kJ)
$\dot{W}$	Power (kW)
$\dot{Z}$	Total Levelized cost ($/h)
z	Rise (m)

Subscript and abbreviations

ASHP	Air source heat pump
AT	Accumulation tank
CELF	Constant escalation leveling factor
COMP	Compressor
CON	Condenser
COP	Coefficient of performance
CRF	Cost restoration factor
e	Exit, electrical, equivalent
EVA	Evaporator
FH	Floor heating
FHC	Floor heating circuit
FHP	Floor heating panel
G	Ground
GHP	Geothermal heat pump

GSHP Ground source heat pump
h Heating
HP Heat pump
HPC Heat pump circuit
i Inlet
k Component
KH Control volume
L Loss, lower value
P Pump
sys System
TV Throttling valve
UGC Underground circuit
UHE Underground heat exchanger

References

Acar MS, Arslan O (2017). Exergo-economic Evaluation of a new drying system Boosted by Ranque-Hilsch vortex tube. Applied Thermal Engineering 124: 1-16. doi: 10.1016/j.applthermaleng.2017.06.010

Acikgoz O, Kincay O, Utlu Z (2014). Determination of the effect of wall heating systems on convective heat transfer coefficient in buildings. Advanced Materials Research 875-877: 1630-36. doi: 10.4028/www.scientific.net/AMR.875-877.1630

Akbulut U, Utlu Z, Kincay O (2016). Exergy, exergoenvironmental and exergoeconomic evaluation of a heat pump-integrated wall heating system. Energy 107: 502-522.

Aldawi F, Alam F, Date A, Alghamdi M, Aldhawi F (2013). A new house wall system for residential buildings. Energy and Buildings 67: 403-18.

Bejan A, Tsatsaronis G, Moran M (1996). Thermal Design and Optimization, John Wiley and Sons Inc., U.S.A.

Buchgeister J (2010). Exergoenvironmental analysis a new approach to support the design for environment of chemical processes. Chemical Engineering Technology 33 (4): 593-602. doi: 10.1002/ceat.201000006

Dincer I, Rosen MA (2013). Exergy: Energy, Environment and Sustainable Development, Elsevier Science, 2nd Edition. doi: 10.1016/C2010-0-68369-6

Dobrota CT, Carpa R, Butiuc-Keul A (2021). Analysis of designs used in monitoring crop growth based on remote sensing methods. Turkish Journal of Agriculture and Forestry 45: 730-742. doi: 10.3906/tar-2012-79

Erbay Z, Hepbasli A (2017). Assessment of cost sources and improvement potentials of a ground source heat pump food drying system through advanced exergoeconomic analysis method. Energy 127: 502-515. doi: 10.1016/j.energy.2017.03.148

Esen H, Inalli M, Esen M, Pihtili K (2007). Energy and exergy analysis of a ground-coupled heat pump system with two horizontal ground heat exchangers. Building and Environment 42: 3606-3615.

Ghorbani Sh, Khoshgoftar-Manesh MH, Nourpour M, Blanco-Marigorta AM (2020). Exergoeconomic and exergoenvironmental analyses of an integrated SOFC-GT-ORC hybrid system. Energy 206: 118151. doi: 10.1016/j.energy.2020.118151

Goedkoop M, Spriensma R (2001). Eco-indicator 99 Methodology report. PRé Consultants b.v., Amersfoort, The Netherlands.

Harjunowibowo D, Omer S A, Riffat S B (2021). Experimental investigation of a ground-source heat pump system for greenhouse heating–cooling. International Journal of Low-Carbon Technologies 16 (4): 1529-1541.

Hepbasli A, Utlu Z (2004). Evaluating the Energy Utilization Efficiency of Turkey's Renewable Energy Sources during 2001. Renewable and Sustainable Energy Reviews 8 (3): 237-255.

Hepbasli A (2011). A comparative investigation of various greenhouse heating options using exergy analysis method. Applied Energy 88: 4411-4423.

Hepbasli A (2013). Low exergy modelling and performance analysis of greenhouses coupled to closed earth-to-air heat exchangers (EAHEs), Energy and Buildings 64: 224-230.

Hu R, Niu JL (2012). A review of the application of radiant cooling & heating systems in mainland China, Energy and Buildings 52: 11–19.

Imanari T, Omori T, Bogaki K (1999). Thermal comfort and energy consumption of the radiant ceiling panel system. Comparison with the conventional all-air system. Energy and Buildings 30: 167–175. doi: 10.1016/S0378-7788(98)00084-X

Jia Y, Wang C, Zhang C, Li W (2017). Numerical Modelling of Radiation-Convection Coupling of Greenhouse Using Underfloor Heating. Open Journal of Fluid Dynamics 7: 448–461.

Karmann C, Schiavon S, Bauman F (2017). Thermal comfort in buildings using radiant vs. all-air systems: a critical literature review. Building and Environment 111: 123–131.

Lohani SP, Schmidt D (2010). Comparison of Energy and Exergy Analysis of Fossil Plant, Ground and Air Source Heat Pump Building Heating System. Renewable Energy 35: 1275-1282.

Mehrabadi ZK, Boyaghchi FA (2019). Thermodynamic, economic and environmental impact studies on various distillation units integrated with gasification-based multi-generation system: Comparative study and optimization. Journal of Cleaner Production 241: 118333. doi:10.1016/j.jclepro.2019.118333

Meyer L, Tsatsaronis G, Buchgeister J, Schebek L (2009). Exergoenvironmental analysis for evaluation of the environmental impact of energy conversion systems. Energy 34: 75-94.

Montazerinejad H, Ahmadi P, Montazerinejad Z (2019). Advanced exergy, exergoeconomic and exergoenvironmental analyses of a solar based Trigeneration energy system. Applied Thermal Engineering 152: 666–685. doi: 10.1016/j.applthermaleng.2019.01.040

Morosuk T, Tsatsaronis G (2008). A new approach to the exergy analysis of absorption refrigeration machines. Energy 33: 890-907. doi: 10.1016/j.energy.2007.09.012

Morosuk T, Tsatsaronis G (2009). Advanced exergetic evaluation of refrigeration machines using different working fluids. Energy 34: 2248-2258.

Morosuk T, Tsatsaronis G (2019). Advanced exergy-based methods used to understand and improve energy-conversion systems. Energy 169: 238-46.

Mousavi SA, Mehrpooya M (2020). A comprehensive exergy-based evaluation on cascade absorption compression refrigeration system for low temperature applications - exergy, exergoeconomic, and exergoenvironmental assessment, Journal of Cleaner Production 246: 119005. doi: 0.1016/j.jclepro.2019.119005

Myhren JA, Holmberg S (2008). Flow patterns and thermal comfort in a room with panel, floor and wall heating. Energy and Buildings 40: 524-36.

Okamoto S, Kitora H, Yamaguchi H, Oka T (2010). A simplified calculation method for estimating heat flux from ceiling radiant panels. Energy and Buildings 42: 29–33. doi: 10.1016/j.enbuild.2009.07.007

Ozgener O, Hepbasli A (2005). Performance analysis of a solar assisted ground source heat pump system for green house heating: an experimental study. Building and Environment 40: 1040-1050.

Rhee KN, Kim KW (2015). A 50 year review of basic and applied research in radiant heating and cooling systems for the built environment. Building and Environment 91: 166–190.

Shirazi A, Aminyavari M, Najafi B, Rinaldi F, Razaghi M (2012). Thermal economic environmental analysis and multi-objective optimization of an internal-reforming solid oxide fuel cellegas turbine hybrid system. International Journal of Hydrogen Energy 37 (24): 19111-24.

Stetiu C (1999). Energy and peak power savings potential of radiant cooling systems in U.S. commercial buildings. Energy and Buildings 30: 127–138. doi: 10.1016/S0378-7788 (98)00080-2

Temir G, Bilge D (2004). Thermodynamic analysis of a trigeneration system. Applied Thermal Engineering 25: 411-422.

Tsatsaronis G, Morosuk T (2016). Advanced exergy-based methods used to understand and improve energy-conversion systems, *CPOTE-2016:* proceedings of the 4th international conference on contemporary problems of thermal engineering; September-14-16, The Silesian University of Technology Institute of Thermal Technology: 75-89, Katowice, Poland.

Tsatsaronis G, Morosuk T (2008). A general exergy-based method for combining a cost analysis with an environmental impact analysis. Part I - theoretical development. In: IMECE 2008 Proc. Int. Mech. Eng. Congress. Expo, Boston, Massachusetts, USA.

Tsatsaronis G, Morosuk T (2009). Understanding and improving energy conversion processes with the aid of exergy-based methods. In: 1st Int. Exergy, life cycle assessment, Sustain. Work. Symposium. Nisyros, Greece.

Unal F, Temir G (2014). Exergoeconomic Analysis of the Ground Source Heat Pump for Cooling Season in the Mardin Province. Sigma Journal of Engineering and Natural Sciences 32: 477-488.

Unal F, Temir G, Köten H (2018). Energy, exergy and exergoeconomic analysis of solar-assisted vertical ground source heat pump system for heating season. Journal of Mechanical Science and Technology 32 (8): 3929-3942.

Ünal İ, Topakci M, Canakci M, Karayel D, Yilmaz E et al. (2021). Development of a mobile robot-based combined sensor platform to determine the correlation between soil penetration resistance and electrical conductivity. Turkish Journal of Agriculture and Forestry 45: 365-379. doi: 10.3906/tar-2007-43

Vangtook P, Chirarattananon S (2010). An experimental investigation of application of radiant cooling in hot humid climate. Energy and Buildings 42: 29–33. doi: 10.1016/j.enbuild.2009.07.007

Yazici H (2011). Determination of Annual Heat Requirement, Fuel Cost and Emission Amount of a Building in Denizli Province According to TS 825 Calculation Method, Selcuk University Journal of Social and Technical Research 1 (2): 29-38 (In Turkish).

Zhang C, Pomianowski M, Heiselberg P, Yu T (2020). A review of integrated radiant heating/cooling with ventilation systems-Thermal comfort and indoor air quality. Energy & Buildings 223: 110094.

Zhao K, Liu XH, Jiang Y (2016). Application of radiant floor cooling in large space buildings - a review, Renewable & Sustainable Energy Reviews 55: 1083–1096.